

General Disclaimer

One or more of the Following Statements may affect this Document

- This document has been reproduced from the best copy furnished by the organizational source. It is being released in the interest of making available as much information as possible.
- This document may contain data, which exceeds the sheet parameters. It was furnished in this condition by the organizational source and is the best copy available.
- This document may contain tone-on-tone or color graphs, charts and/or pictures, which have been reproduced in black and white.
- This document is paginated as submitted by the original source.
- Portions of this document are not fully legible due to the historical nature of some of the material. However, it is the best reproduction available from the original submission.

NASA TM X- 71064

IRON LINE EMISSION FROM A HIGH TEMPERATURE PLASMA IN Cas A

S. H. PRAVDO
R. H. BECKER
E. A. BOLDT
S. S. HOLT
R. E. ROTHSCHILD
P. J. SERLEMITSOS
J. H. SWANK

JANUARY 1976



GODDARD SPACE FLIGHT CENTER
GREENBELT, MARYLAND

(NASA-TM-X-71064) IRON LINE EMISSION FROM A
HIGH TEMPERATURE PLASMA IN Cas A (NASA)
16 p HC \$3.50 CSCL 03A

N76-18008

Unclas
14852

G3/89

Iron Line Emission from a High Temperature

Plasma in Cas A

S. H. PRAVDO*, R. H. BECKER[†], E. A. BOLDT, S. S. HOLT
R. E. ROTHCHILD, P. J. SERLEMITSOS, J. H. SWANK[†]
NASA/Goddard Space Flight Center
Greenbelt, Maryland 20771

ABSTRACT

The x-ray spectrum of Cassiopeia A was observed for several days by the GSFC proportional counter experiment on board OSO-8. The high energy (> 5 keV) data are fit well by a thermal spectrum with $kT = 3.9^{+0.9}_{-0.4}$ keV. A narrow iron line which is predicted by the thermal model is also observed, centered at $6.66^{+0.14}_{-0.16}$ keV with an equivalent width of 1270^{+175}_{-40} eV. The low energy (2-5 keV) data show an excess over the high temperature component which is consistent with the presence of an additional low temperature thermal component with $kT \leq 0.7$ keV and $N_H \sim 10^{22}$ atoms cm^{-2} . Iron abundance in the source relative to normal cosmic abundance is discussed, as in the relation of this observation to shock wave and multi-component thermal models for supernova remnants.

*Work supported by U. of Maryland Grant 21-002-316
[†]NAS/NRC Research Associate

I. Introduction

Cassiopeia A has the highest intrinsic and apparent X-ray luminosity of all known supernova remnants except for the Crab Nebula. Optical (van den Bergh and Dodd 1970), radio (Rosenberg 1970 a, b), and X-ray (Fabian et al. 1973) observations have shown this most recent supernova (100-400 years old) to be an extended source. In this Letter we report on the measurement of the X-ray spectrum of Cas A with a proportional counter on board Orbiting Solar Observatory 8 (OSO-8).

II. Experiment

OSO-8 was launched June 21, 1975. It carries seven experiments. The two prime solar experiments are mounted on the spacecraft sail and five others on the wheel, the spinning portion of the spacecraft. One of this latter group is the GSFC Cosmic X-ray Spectroscopy experiment (CXS). It consists of three multi-anode, multi-layer gas proportional counters in or near alignment with the spacecraft spin axis.

The detector relevant to this observation is a xenon-filled counter featuring an additional gas volume of neon-propane adjacent to the collimator to guard against precipitating electrons entering via the collimator. This detector has a 5 degree circular field of view centered about the positive spin axis. The view is periodically occulted by the pointed solar instruments and by two occultation shields mounted under the spacecraft sail. These are designed to provide a measure of the intrinsic detector background. Data from this detector are binned by onboard logic that distinguishes whether the field of view is open or occulted. Other relevant features include a

net area of 237 cm^2 , a transmission window of two .001" mylar sheets in addition to the neon-propane gas in the anticoincidence volume, and an onboard Am^{241} calibration source.

The observation was carried out during the period July 17-26. The results presented here are from "Quick Look" data corresponding to about 10% of all data. Background measurements were made just before as well as after Cas A was in the field of view. The background in this region of the sky was found to be very stable.

III. Results

The excellent statistics allow a multi-parameter fit to the Cas A spectrum from which meaningful model-building can proceed. First the high energy ($> 7 \text{ keV}$) points alone were fit, agreeing equally well with a power law with number index $4.5 \pm .5$ and a thermal spectrum with $kT = 3.2^{+1.0}_{-.6} \text{ keV}$, where the errors quoted refer to acceptability at 90% confidence. These confidence intervals are calculated by allowing the minimum acceptable value for χ^2 to vary by an amount consistent with the number of parameters in the model (Lampton et al. 1975). The analytical form used to represent a thermal spectrum is

$$\frac{dN}{dE} = C g(E, kT) \exp(-E/kT)/E \quad (1)$$

with C a normalization constant and $g(E, kT) = (E/kT)^{-0.4}$ an approximate form for the Gaunt factor. This spectral form (equation 1) adequately approximates the continuum contribution from an isothermal optically thin thermal plasma calculated in various numerical models (see below). The model in equation 1 can be tested against the data either by folding it through the detector response function (forward direction) or by

multiplying it by spectral dependent channel-by-channel efficiencies (backward direction) when good fits are obtained. These two methods converge to the same best fit parameters.

Next, the energy region around 7 keV is included in the analysis. An acceptable best fit is found by including a narrow line centered at $6.66^{+0.14}_{-0.16}$ keV. When the detector resolution was introduced as a free parameter and varied, the best fit was found at the resolution value previously determined by calibration (FWHM 1.1 keV at 6.66 keV). The $2p \rightarrow 1s$ transitions in thermally excited Fe^{+25} and Fe^{+24} would form a feature with these characteristics. The iron line has an equivalent width of 1270^{+175}_{-40} eV, while the channel energy width in the CXS is $\sim .6$ keV. Accordingly, the line to continuum ratio in the channel centered at 6.7 keV, where most ($\sim 45\%$) of the line photons fall, is $0.96^{+0.12}_{-0.04}$. Some evidence is seen for an enhancement around 8.2 keV, where lines from $np \rightarrow 1s$ ($n > 2$) of Fe^{+25} and Fe^{+24} are expected at a lower level.

The thermal spectrum and iron line, which yield an acceptable fit to data points above 6 keV, do not fully account for the lower energy data. The residuals are fit well with an additional low temperature thermal with $kT \leq .7$ keV and $N_H \sim 10^{22}$ atoms cm^{-2} . The contribution of this component changes the best fit parameter for the high temperature component, which now becomes $3.9^{+0.9}_{-0.4}$ keV.

We present the data and best fit model in the first two figures. Figure 1a shows the data as points and bars representing the statistical errors, superimposed on a histogram of the CXS response when the input spectrum is the best fit model described above. A χ^2 value of 23

with 19 degrees of freedom is obtained. The iron line is represented as a Gaussian centered at 6.66 keV with FWHM \ll 1.1 keV. If the FWHM of the Gaussian is increased to be \approx 1.1 keV the acceptable fit is lost. Since we were able to find convergent best fit models, accurate channel-by-channel efficiencies were calculated. Figure 1b shows the inferred incident spectrum obtained by analysis in the backward direction making use of the efficiencies described above.

In Figure 2 the observed feature around 6.7 keV is displayed by folding the best fit thermal continuum through the detector response function and subtracting this resultant from the data. The width and shape of this feature are consistent with detector broadening of a narrow line. Although the observed line falls in several channels, the analysis described above allows us to conclude that with better resolution, we would have observed it in only one channel (Fig. 1b).

In contrast to the complex spectrum of Cas A, Figure 3 shows the spectra of two sources observed at different times by the same detector. The same analysis procedure was used to obtain these inferred spectra. The Crab Nebula is a featureless relatively flat power law while Nova Monocerotis 1975 exhibits an equally featureless but steep thermal spectrum.

IV. Discussion

Cas A has no observable pulsed emission (Holt et al. 1973), and Fabian et al. (1973) did not find a central intensity enhancement. Thus there is no evidence for a pulsar in the remnant. In the Crab Nebula the emission is dominated by processes originating at the pulsar. This

featureless power law (Fig. 3) due to synchrotron radiation masks any possible thermal emission from the remnant (but see Toor et al. 1975). Without a strong pulsar, a complex thermal spectrum is evident from Cas A. Charles et al. (1975) fit their observation of Cas A to a two temperature thermal spectrum with $kT = 2.6$ keV and 0.7 keV. A thermal spectrum with temperature 1.4 keV was measured by Hill et al. (1975) with increased silicon and decreased iron abundance. Serlemitsos et al. (1973) observed Cas A with a xenon detector similar to the OSO-8 CXS. They interpreted the 2-20 keV spectrum as a power law in photon number with a doppler broadened line feature centered around 6.9 keV due to charge exchange between Fe^{+25} and Fe^{+26} cosmic rays and ambient interstellar matter. Their next most acceptable fit was a spectrum consisting of two thermal components. All report absorption consistent with $N_H \approx 10^{22}$ atoms cm^{-2} .

In the present measurement improved statistics allow us to resolve this spectrum further. The feature around 6.7 keV persists, but is now seen to be narrow, broadened only to an extent consistent with the instrumental resolution at this energy (1.1 keV FWHM). This can be interpreted as thermal emission lines from iron. Although the high energy ($E > 7$ keV) data is consistent with a steep power law (number index of 4.5), the presence of narrow iron lines strongly suggests a thermal source of temperature $kT = 3.9$ keV which also yields an acceptable fit for high energies. Around this temperature iron is most efficient in emitting K X-rays. For temperatures much below this, the highly ionized states are not populated and for higher temperatures the nuclei are normally fully stripped. However, in the 'standard'

supernova shock wave model presented in Gorenstein et al. (1974) (and references cited therein) the electrons and ions in the plasma behind the shock wave may be at different temperatures. The time needed for the ions and electrons to reach thermal equilibrium via coulomb collisions is long compared with the lifetime of the Cas A remnant. The electron temperature is observed directly from the X-ray spectrum while the ion temperature is deduced from the velocity of the optical filaments and found to be ~ 30 times higher-about 40 keV. In thermal equilibrium at this temperature iron nuclei are stripped of atomic electrons but in a non-steady state situation (cf. Kafatos and Tucker 1972) the ionization state could be less, leading to anomalous line emission. Alternatively, McKee (1974) proposed electrodynamic coupling as a mechanism to bring the ions and electrons into thermal equilibrium much more quickly. At the electron temperature, iron would emit intense line emission in the steady state. In what follows we assume this last condition.

The total energy flux in the iron lines can be compared to the continuum flux to obtain an estimate for iron abundance in the plasma at this temperature. Several model calculations have been performed for optically thin plasmas in this temperature range. Among them are Tucker and Koren (TK) (1971), Felten, Rees, and Adams (FRA) (1972), and Raymond and Smith (RS) (1975). This last work includes Gaunt factor calculations of Mewe (1972), line emission contributions from dielectronic recombinations, and new calculations of ionization equilibrium. Table 1 displays results using the preceding models. The first two columns are inferred equivalent widths and detector-dependent line to continuum ratios respectively, with 'cosmic' abundances

TABLE I

MODEL	e.w. (eV)	L/C	$n_{\text{Fe}}/n_{\text{Fe}}^{\text{COSMIC}}$
TK	800	0.5	1.9
FRA	870	0.6	1.6
RS	1800	1.5	0.64

(i.e. logarithmic iron abundance of 7.6 relative to hydrogen at 12.0.)
The third column shows the iron abundance enhancement factor needed to produce the observed line to continuum ratio.

The general conclusion we reach from Table 1 is that normal cosmic iron abundance is adequate to explain this observation. If the lower ratio estimates from the first two models are correct, iron may be enhanced in Cas A over cosmic abundances as is to be expected if heavy elements are synthesized in highly evolved stars. In the early stage of the standard model the mass ejected by the supernova, M_e , is large compared to the interstellar matter swept up,

$$M_e \geq \frac{4}{3} \pi r^3 m_p N_0 \quad (2)$$

assuming a spherical expanding shell into a homogeneous interstellar medium of number density N_0 . The radiating plasma matter will be more characteristic of evolved supernova constituents than of interstellar matter. The shell luminosity is given by Gorenstein et al. (1974) as

$$L_x \approx 5 \times 10^{56} N_0^2 P(T) R^3 \text{ erg/s} \quad (3)$$

where $N_0^2 P(T)$ is the emissivity of the plasma and R is measured in parsecs. In the present observation the 3.9 keV component has an intrinsic luminosity of $7.3 \times 10^{35} \text{ erg s}^{-1}$ and together with the known values of $P(T)$ and R , we determine $N_0 = 4.5 \text{ cm}^{-3}$. This gives from equation (2), $M_e \geq 4.6 M_\odot$. The value for the density is somewhat lower than previous estimates (Gorenstein et al. 1974) because only the flux from the high temperature component is considered.

If the higher estimate for line to continuum ratio of KS is correct than iron is not enhanced in Cas A. Either iron was not over-abundant in the evolved star or Cas A is in a later stage than assumed in the preceding and M_e is less than the ambient mass swept up. However this possibility does indicate that even cosmic abundance of iron should be readily observable by our and similar detectors via its line emission signature in hot optically thin gases.

The low temperature component of the Cas A spectrum was observed as an excess in low energy channels over the high temperature component. The observed $kT \leq .7$ keV and $N_H \approx 10^{22}$ is similar to that in previous observations. Because of the uncertainties in the continuum contributions of the two components and the detector efficiency cutoff near 2 keV we are unable to estimate the silicon line contribution or comment on the need for enhanced silicon abundance.

Supernova models with more than one thermal component have been applied to Cas A. McKee (1974) associates a high temperature thermal with the outward propagating supernova shock and a low temperature thermal with an inward propagating reverse shock. Recent results of Charles (1975) indicate a spatial separation between components, with a low energy excess concentrated toward the center of the remnant. Chevalier (1975) attributes different components to hot gas as well as to the denser flocculi moving away from the explosion site. Both models suggest a component with $kT \geq 20$ keV. If this high temperature

component is present in addition to the observed 3.9 keV plasma, then between 5-50 keV the power in the former is at least a factor of 5 below the power in the latter.

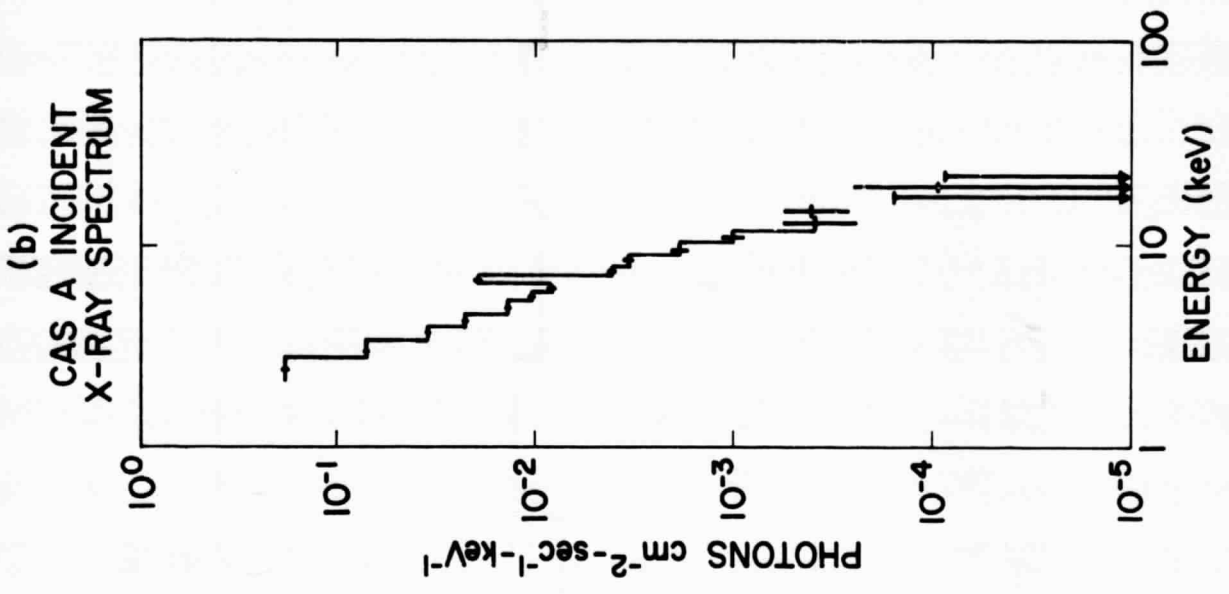
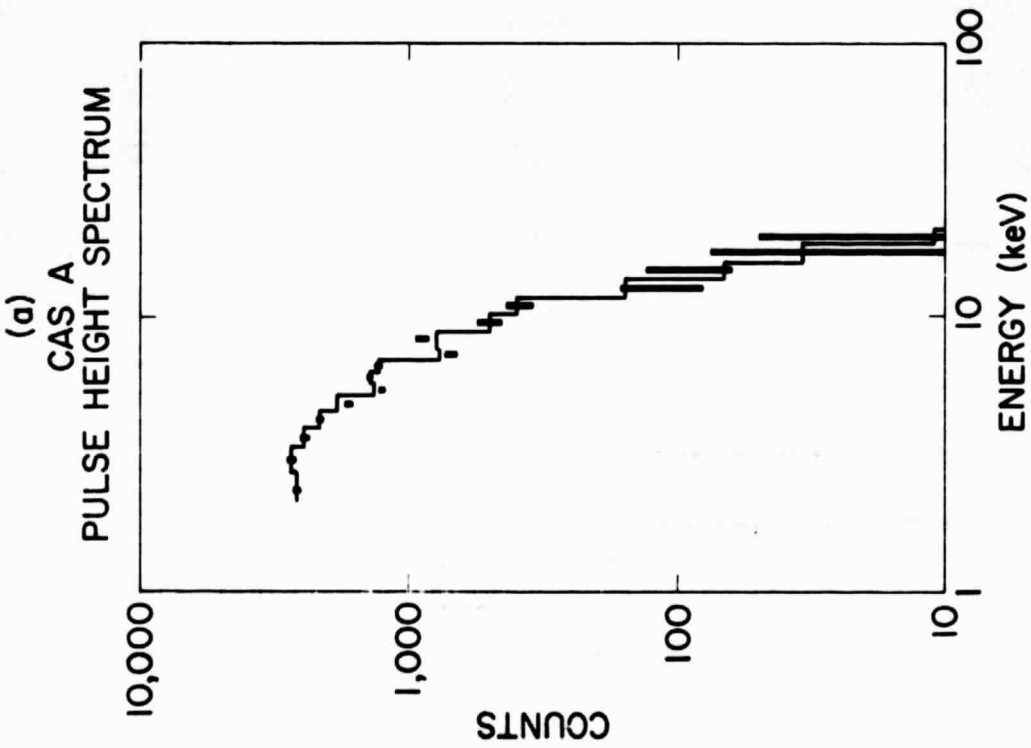
We would like to thank the people involved in the GSFC experiment as well as the OSO project. In the construction and testing of the experiment we thank C. Glasser, F. Birsa, T. Kaminski, J. Saba, S. Jones, and E. Mundy. We also thank the delta launch crew at Cape Canaveral, and Hughes Aircraft Co. for the excellent orbiting platform from which these observations were carried out.

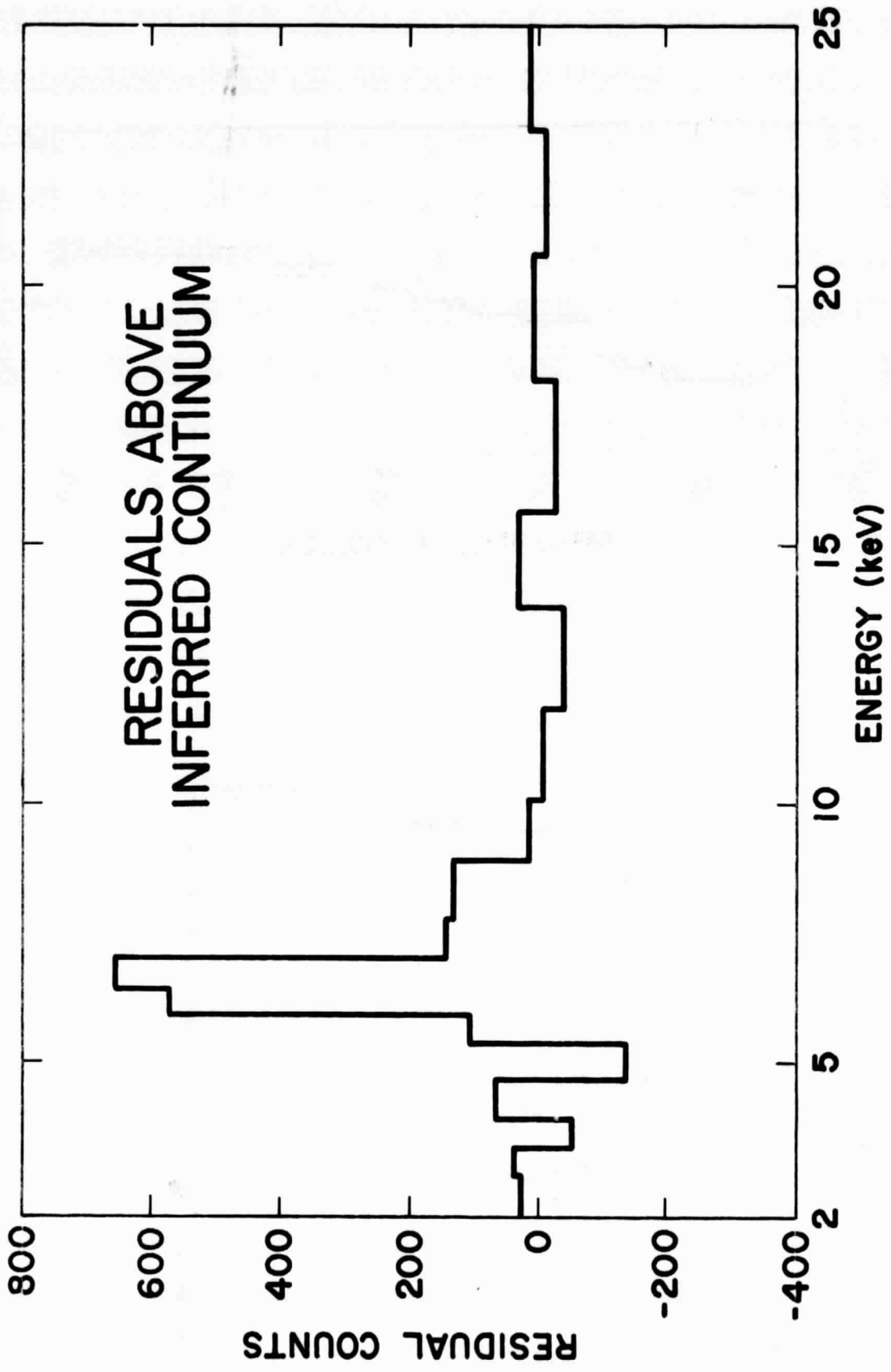
References

- Bergh, S., van den, and Dodd, W. W. 1970, Ap. J., 162, 485.
- Brown, R. L., and Gould, R. J. 1970, Phys. Rev., D1, 2252.
- Charles, P. A. 1975, private communication.
- Charles, P. A., Culhane, J. L., Zarnecki, J. C., and Fabian, A. C.
1975, Ap. J. (Letters), 197, L61.
- Fabian, A., Zarnecki, J., and Culhane, J. 1973 Nature Phys. Sci.,
242, 18.
- Felten, J. E., Rees, M. J. and Adams, T. F. 1972, Astr. and Ap., 21,
139.
- Gorenstein, P., Harnden, F. R., Tucker, W. H. 1974, Ap. J., 192, 661.
- Hill, R. W., Burginyon, G. A., and Seward, F. D. 1975, Ap. J., 200,
p. 158.
- Holt, S. S., Boldt, E. A., Brisken, A. F., and Serlemitsos, P. J.
1973, Ap. J. (Letters), 180, L69.
- Kafatos, M. C. and Tucker, W. 1972 Ap. J., 175, 837.
- Lampton, M., Margon, B., and Bowyer, S. 1975, preprint.
- McKee, C. F. 1974, Ap. J., 188, 335
- Mewe, R. 1972, Astr. and Ap., 20, 215.
- Raymond, J. and Smith, B. 1975, private communication.
- Rosenberg, I. 1970a, M.N.R.A.S., 147, 215.
———1970b, ibid. 151, 109.
- Serlemitsos, P. J., Boldt, E. A., Holt, S. S., Ramaty, R., and
Brisken, A. F. 1973 Ap. J. (Letters), 184, 1.
- Toor, A., Palmieri, T. M., and Seward, F. D. 1975, Buil. A.A.S., 7, 456.
- Tucker, W. H. and Koren, M. 1971, Ap. J., 168, 283.

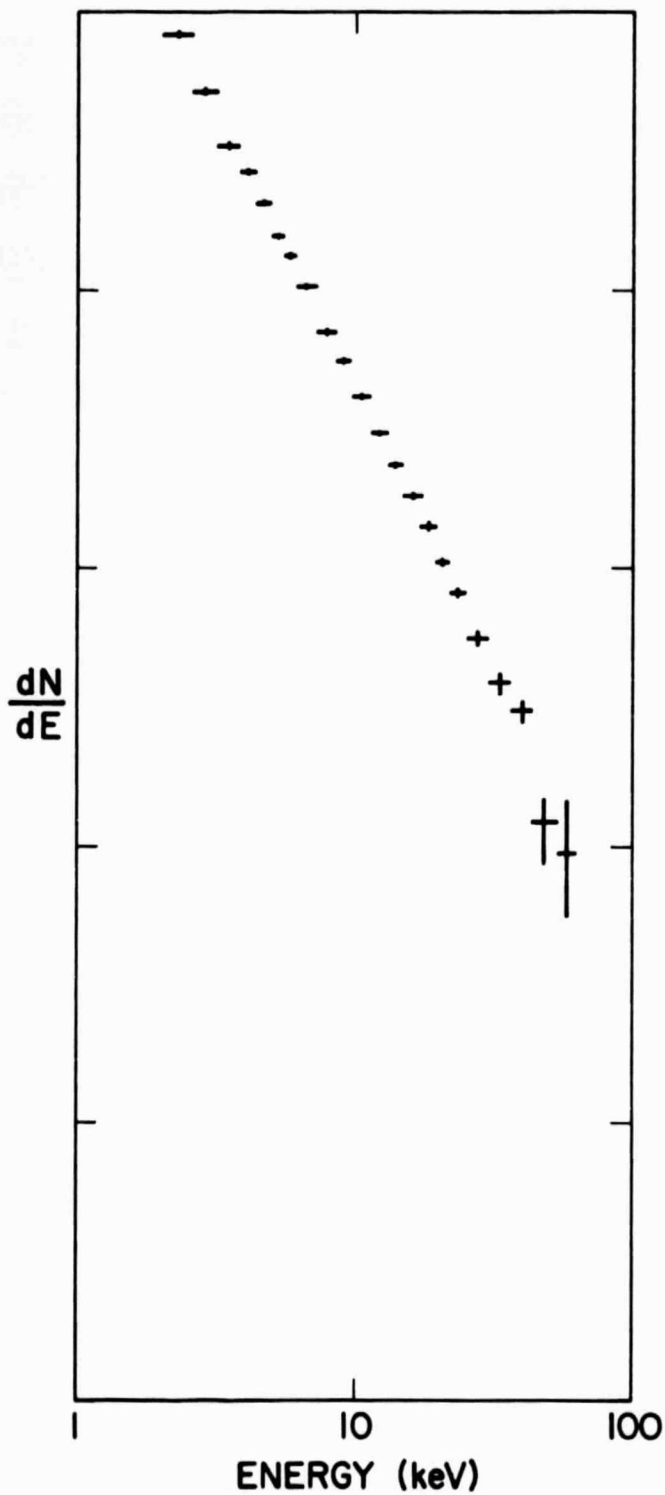
Figure Captions

- 1(a). The points and heavy bars are the observed counts in each energy bin with their statistical errors. The histogram results from folding the best fit model described in the text through the detector response function.
- (b). The inferred incident spectrum obtained by dividing the data by the true channel-by-channel efficiencies.
2. Residuals as a function of energy, obtained by subtracting from the data the best fit continuum folded through the detector response function.
3. The spectra of (a) the Crab and (b) Nova Monocerotis 1975 obtained with the same detector which observed Cas A but at different times. The vertical scale is photons $\text{cm}^{-2}\text{sec}^{-1}\text{keV}^{-1}$ with different normalizations for the two spectra.





(a)
OSO-8
CRAB
11/6/75



(b)
OSO-8
NOVA MONOCEROTIS 1975
10/1/75

